UV Resonance Raman Ground and Excited State Studies of Amide and Peptide Isomerization Dynamics

Pusheng Li, X. G. Chen,† E. Shulin, and Sanford A. Asher*

Contribution from the Department of Chemistry, University of Pittsburgh, Pittsburgh, Pennsylvania 15260

Received June 19, 1996[⊗]

Abstract: We report the first measurements of the activation barrier for ground state trans−cis isomerization of secondary amides. We measured activation barriers of $E_a = 13.8 \pm 0.8$ kcal/mol for aqueous solutions of *N*-methylacetamide (NMA) and $E_a = 11.0 \pm 0.7$ kcal/mol for glycylglycine (Gly-Gly). These activation barriers were determined from the temperature dependence of the ground state isomerization rates, which were measured by using UV resonance Raman to monitor the relative populations of the cis and trans amides as the sample solutions were translated through a 206.5 nm CW laser beam. Photon absorption causes the normally trans form to isomerize to the cis form. We developed a photochemical model to relate the measured relative Raman intensities to the ground state isomerization rates. We also measured the photochemical isomerization quantum yields, the yields for photochemical degradation, and the cis and trans Raman cross sections and their molar absorptivities. We also measured the temperature dependence of the cis and trans Raman intensities to determine the Gibbs free energy gap between the ground state cis and trans forms of NMA (2.6 ± 0.4 kcal/mol) and Gly-Gly (3.1 ± 0.5 kcal/mol).

Introduction

The importance of the amide functional group as a chemical covalent linkage is amply demonstrated by the fact that the amide peptide bond is the fundamental linkage in peptides and proteins. The geometric constraints imposed by amide linkages, such as the enforced amide planarity, define the conformational freedom of motion for many small molecules as well as for peptides and proteins. Numerous previous experimental studies investigated the geometric constraints of the amide linkage, and recently, numerous theoretical studies examined the torsional barriers to rotation about the C(O)−N amide bond.[1−8] All previous direct measurements of the activation barrier to rotation about this amide bond[9−14] were limited to tertiary amides and methylformamide[15,16] because the previously available methods required significant concentrations of the cis amide form. These studies found barriers which varied from 10 to 27 kcal/mol.

The most interesting amide torsional barriers occur in secondary amides, which have similar bonding and structure to the peptide bonds. Unfortunately, these amides show very small concentrations of the cis form because the cis-form Gibbs free energy is significantly above that of the trans form. The experimental determination of these barriers is especially important because these parameters are required for the accurate molecular modeling of peptides and protein structure and dynamics. However, the theoretical approaches to determining these barriers in water are challenged to the point of unreliability.

In this work we report the development of a new technique to directly measure the activation barriers to ground state isomerization of the secondary amides *N*-methylacetamide (NMA) and glycylglycine (Gly-Gly). This method utilizes the trans to cis photochemical isomerizations of *trans*-NMA and Gly-Gly to populate the cis forms.[17,18] We utilize resonance Raman spectroscopy to kinetically monitor the relative concentrations of the cis and trans forms in order to determine the ground state isomerization rates. Measurements of the temperature dependences of these rates directly determine the activation barriers. The room temperature isomerization rates are slow (ca. 2.3 s^{-1} for NMA).

Experimental Section

NMA and Gly-Gly were purchased from Sigma Chemical Co. and used as received. The aqueous solution samples were prepared at concentrations of 5−7 mM in the presence of 0.5 M $NaClO_4$ used as an internal intensity standard.

The Raman spectra were measured by using a 135° scattering geometry (Figure 1). Excitation of different annular segments of a slowly spinning sample cell results in different translation speeds of the illuminated sample volume through the laser beam. Diffusion of sample molecules out of the illuminated volume during the illuminated interval is negligible, even at the lowest sample volume translation speeds (∼0.4 mm/s, which results in a 0.2 s residence time in the laser beam), for the diffusion constants expected (ca. 10^{-5} cm^2/s).

An air bladder inside the sample cell buffered the sample volume changes during sample temperature alterations. The sample temperature was controlled by a Omega CN380 temperature controller and heating tape wrapped around the sample cell cover. Hot air was blown on the sample cell front surface to maintain a uniform temperature distribution.

* Author to whom correspondence should be addressed. Phone: (412) 624-8570. FAX: (412) 624-0588. E-mail: asher+@pitt.edu.

† Present address: Section on Metabolic Analysis and Mass Spectrometry, NICHD, National Institute of Health, 10 Center Drive, MSC 1580, 6C208, Bethesda, MD 20892.

⊗ Abstract published in *Advance ACS Abstracts,* January 1, 1997.

(1) Christensen, D. H.; Kortzeborn, R. N.; Bak, B.; Led, J. J. *J. Chem. Phys.* **1970**, *53*, 3912.
(2) Perricaudet, M.; Pullman, A. *J. Pept. Protein Res.* **1973**, *5*, 99.
(3) Nalewajski, R. F. *J. Am. Chem. Soc.* **1978**, *100*, 41.
(4) Hoesterey, B.; Neely, W. C.; Worley, S. D. *Chem. Phys. Lett.* **1983**, *94*, 311.
(5) Radom, L.; Riggs, N. V. *Aust. J. Chem.* **1980**, *33*, 249.
(6) Wiberg, K. B.; Laidig, K. E. *J. Am. Chem. Soc.* **1987**, *109*, 5935.
(7) Knight, E. T.; Allen, L. C. *J. Am. Chem. Soc.* **1995**, *117*, 4401.
(8) Wiberg, K. B.; Rablen, P. R. *J. Am. Chem. Soc.* **1995**, *117*, 2201.
(9) Phillips, W. D. *J. Chem. Phys.* **1955**, *23*, 1363.
(10) Sunners, B.; Piette, L. H.; Schneider, W. G. *Can. J. Chem.* **1960**, *38*, 681.
(11) Drakenberg, T.; Forsén, S. *J. Phys. Chem.* **1970**, *74*, 1.
(12) Kamei, H. *Bull. Chem. Soc. Jpn.* **1968**, *41*, 2269.
(13) Berg, U.; Åström, N. *Acta Chem. Scand.* **1995**, *49*, 599.
(14) Clerk, G. R.; Surman, P. W. J.; Taylor, M. J. *J. Chem. Soc., Faraday Trans.* **1995**, *91*, 1523.
(15) LaPlanche, L. A.; Rogers, M. T. *J. Am. Chem. Soc.* **1964**, *86*, 337.
(16) Siddall, T. H.; Stewart, W. E., III; Marston, A. L. *J. Phys. Chem.* **1968**, *72*, 2135.
(17) Song, S.; Asher, S. A.; Krimm, S.; Shaw, K. D. *J. Am. Chem. Soc.* **1991**, *113*, 1155.
(18) (a) Wang, Y.; Purrello, R.; Spiro, T. G. *J. Am. Chem. Soc.* **1989**, *111*, 8274. (b) Wang, Y.; Purrello, R.; Georgiou, S.; Spiro, T. G. *J. Am. Chem. Soc.* **1991**, *113*, 6368.

S0002-7863(96)02058-6 CCC: $14.00

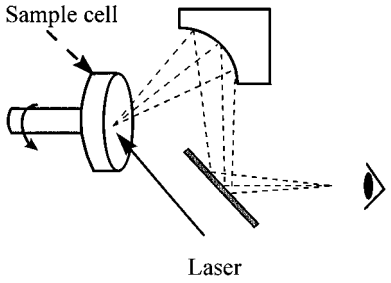

Figure 1. Raman scattering measurement geometry.

Thermocouples monitored the cell temperature, which was constant within ±1.5 K.

The 206.5 nm CW excitation was obtained from an intracavity frequency-doubled Kr^+ laser.[19] This CW 206.5 nm excitation was used for the flowing kinetic studies, which were used to determine the ground state cis to trans isomerization rates and to determine the photodegradation quantum yields. The 208 nm 15 ns pulsed excitation, that was used to determine the photoisomerization quantum yields and the cis amide absorption cross sections, was obtained from a frequency-doubled Lambda Physik 2000 dye laser which used *p*-bis(*o*-methylstyryl)benzene dye. The dye laser was pumped by a 308 nm Lambda Physik Model EMG103 excimer laser operated at 100 Hz with a ca. 16 ns pulse width.[20] The laser power was attenuated by neutral density filters. The scattered light was dispersed by a Spex-1877B Triplemate spectrometer using an 1800 gr/mm grating, and the photons were detected by an Princeton Instruments intensified CCD detector.

We used a classical thermal diffusion model[21] to calculate the likely sample temperature increases which result from the incident tightly focused laser beam excitation. We calculate that less than a 3 K temperature increase occurs. This conclusion is supported by the fact that we did not observe any laser power dependent frequency shifts in the trans amide II and III bands which are well-known to occur with sample temperature changes.[17]

The error in our calculations of ground state isomerization barriers result from the spectral signal−noise ratios, errors in our spectral peak deconvolutions, laser power fluctuations, errors in measurements of the laser beam size, errors derived from our assumptions of a Gaussian band shape, and errors which result from sample temperature fluctuations. We estimate that the error in the measured ground state cis → trans coversion rate, *K*, is about 15%; however, the standard error for the regression is much less. We quote error limits of ±1 standard deviation.

Results and Discussion

We determined the ground state trans to cis isomerization kinetics by measuring the 206 nm resonance Raman spectra of spinning samples of NMA and Gly-Gly; absorption of light transfers state *trans*- and *cis*-NMA or Gly-Gly into their excited states (Figure 2). Ultrafast relaxation transfers these excited molecules back into their trans or cis ground states. The net quantum yield for cis formation is sufficiently high that photoisomerization increases the cis concentration and decreases the trans concentration. We do not know, as yet, whether the photochemical isomerization occurs on an excited state or ground state surface; isomerization may occur within the $\pi\pi^*$ state or within a different intermediate excited state. The photoisomerization mechanism could also be thermal and occur on the ground state surface due to absorption of these high-energy UV photons, which heat the molecule and transiently populate high ground state vibrational levels.

The cis and trans ground states of NMA and Gly-Gly show distinctly different, easily resolved Raman bands. As discussed in the Appendix we can determine the ground state isomerization rates by translating the illuminated sample volume through the 206.5 nm CW excitation beam at different speeds. We determine the ground state isomerization activation barriers by measuring the temperature dependence of these ground state isomerization rates.

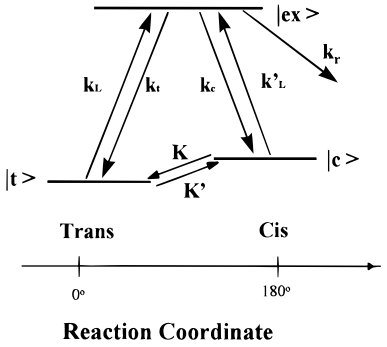

Figure 2. Three-state kinetic model which describes the isomerization dynamics of amides through photochemistry and ground state isomerization. Irreversible photochemical degradation through the excited state is also included.

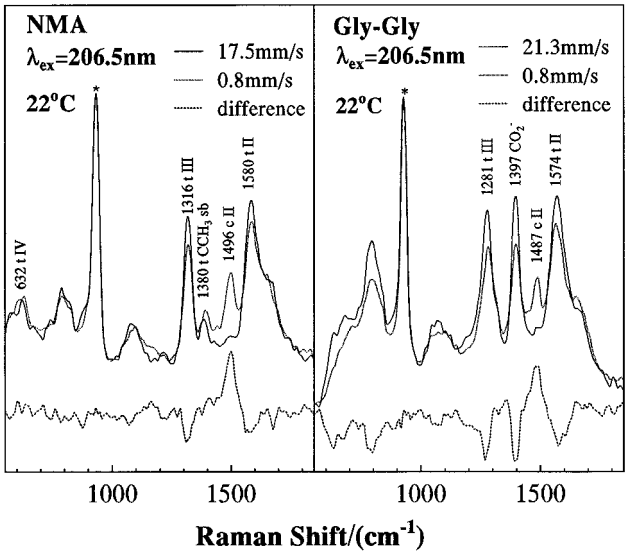

Figure 3. UV Raman spectra (206.5 nm excitation) of *N*-methylacetamide (NMA) and glycylglycine (Gly-Gly) at room temperature at fast and slow sample translation speeds. The band at 932 cm^{-1} is from the $NaClO_4$ (0.5 M) used as an internal intensity standard. The difference spectra are also shown.

Resonance Raman Spectra. Figure 3 shows the 206.5 nm CW room temperature resonance Raman spectra of aqueous NMA and Gly-Gly at fast and slow sample translation speeds and their difference spectra. The 932 cm^{-1} band derives from the perchlorate internal standard, while the bands at ca. 1580 and 1300 cm^{-1} and the shoulder at 1650 cm^{-1} derive from the amide II and III and the amide I bands of the trans forms of NMA and Gly-Gly.[22] The 1380 cm^{-1} *trans*-NMA band derives from the symmetric methyl bending vibration, while the ca. 1400 cm^{-1} band of *trans*-Gly-Gly derives mainly from the symmetric COO^- stretch, which overlaps the $C_\alpha H_2$ symmetric bending vibration.[22]

Photon absorption by the dominantly trans ground state results in photoisomerization to the cis form. The ca. 1490 cm^{-1} bands which appear at low sample translation rates derive from the cis amide II bands of NMA and Gly-Gly. The slow sample translation speed spectra show decreased trans amide bands intensities, while the cis amide II band intensities increase. The cis amide II band intensity increases shown by NMA and Gly-Gly at 1496 and 1487 cm^{-1} are larger than the trans amide II and III band intensity decreases, due to the known larger Raman cross sections of the *cis*-NMA amide II bands due to the red-shifted cis $\pi \rightarrow \pi^*$ electronic transition.[17]

(19) Holtz, J. S. W.; Bormett, R. W.; Chi, Z.; Cho, N.; Chen, X. G.; Pajcini, V.; Asher, S. A.; Spinelli, L.; Owen, P.; Arrigoni, M. *Appl. Spectrosc.* **1996**, *50*, 1459.
(20) Cho, N.; Asher, A. S. *Biospectroscopy* **1996**, *2*, 71.
(21) Li, P.; Champion, P. M. *Biophys. J.* **1994**, *66*, 430.

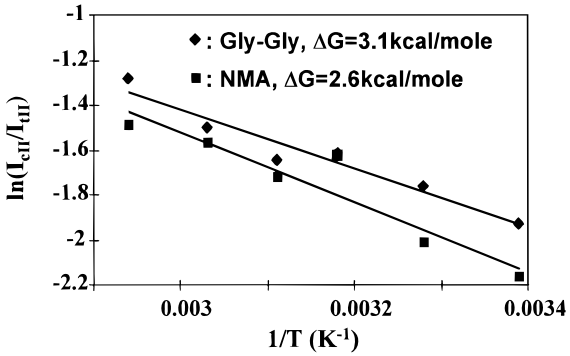

Figure 4. Natural log of the ratio of the cis amide II to the trans amide II band Raman intensities as functions of $1/T$. The solid lines are the best linear least-square fit whose slope give the Gibbs free energy gap between the cis and trans amide forms.

Cis-Form Raman Cross Sections. We determined the Raman cross sections of *cis*-NMA and *cis*-Gly-Gly in two ways. The most direct and accurate way was by ratioing the decreased trans amide II and III band intensities to the increased cis amide II band intensity, since we determined that the degradation quantum yield was small (vide infra). This yields 206.5 nm Raman cross sections of 0.8 ± 0.1 b/(molecule sr) for *cis*-NMA and 4.6 ± 0.7 b/(molecule sr) for *cis*-Gly-Gly. These cis Raman cross sections are 11- and 21-fold larger than those for *trans*-NMA (0.07 ± 0.01 b/(molecule sr)) and Gly-Gly (0.22 ± 0.03 b/(molecule sr)),[22c] respectively. The Raman cross section of Gly-Gly is larger than that of NMA due to the additional resonance enhancement from the Gly-Gly carboxylate to amide charge transfer.[22]

A less accurate approach uses measurements of the temperature dependence of the cis amide II Raman intensities. The cis−trans population ratio is

$$\frac{N_{\text{cis}}}{N_{\text{trans}}} = \frac{I_{\text{R}}^{\text{cis}}/\sigma_{\text{R}}^{\text{cis}}}{I_{\text{R}}^{\text{trans}}/\sigma_{\text{R}}^{\text{trans}}} = \exp(-\Delta G/RT) \qquad (1)$$

where $I_{\text{R}}^{\text{cis}}$ and $I_{\text{R}}^{\text{trans}}$ are Raman scattering intensities from cis and trans forms and $\sigma_{\text{R}}^{\text{cis}}$ and $\sigma_{\text{R}}^{\text{trans}}$ are Raman cross sections of cis and trans forms. Equation 1 can be rewritten as

$$\ln\left(\frac{I_{\text{R}}^{\text{cis}}}{I_{\text{R}}^{\text{trans}}}\right) = \ln\left(\frac{\sigma_{\text{R}}^{\text{cis}}}{\sigma_{\text{R}}^{\text{trans}}}\right) - \frac{\Delta G}{R}\left(\frac{1}{T}\right) \qquad (2)$$

and we can extract the ratio of the Raman cross sections of the cis and trans forms from the intercept of the $\ln(I_{\text{R}}^{\text{cis}}/I_{\text{R}}^{\text{trans}})$ vs $1/T$ plot, given that we have measured the cross sections of the trans species. This approach gives similar values but with larger error limits.

Cis and Trans Form Ground State Energy Difference. We can directly determine the Gibbs free energy difference between the ground state cis and trans forms by examining the temperature dependence of the relative cis and trans Raman intensities at low excitation fluxes. Figure 4 plots the natural log of the ratio of the cis to trans amide II intensities versus $1/T$ for NMA and Gly-Gly. The solid lines are the linear least-squares best fits, whose slope are $\Delta G/R$. $\Delta G = 2.6 \pm 0.4$ kcal/mol for NMA, and $\Delta G = 3.1 \pm 0.5$ kcal/mol for Gly-Gly; these results are close to previous theoretical[23,24] and experimental[25] determinations.

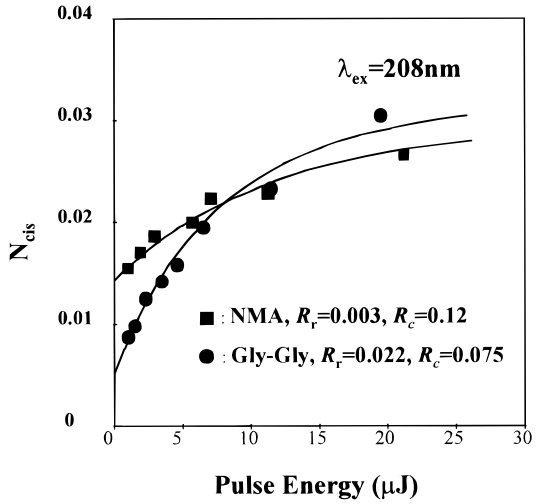

Figure 5. Concentration of the cis form as a function of pulse laser energy for NMA and Gly-Gly at 208 nm. The solid curves are the best fit to eq A.3, where we approximate K and $K' = 0$.

Photoisomerization Quantum Yields. Figure 5 shows the dependence of the concentrations of *cis*-NMA and Gly-Gly as a function of the 208 nm pulse excitation energy. The cis concentrations were determined from the Raman scattering intensities of the 1492 and 1487 cm^{-1} cis amide II bands of NMA and Gly-Gly. The solid curves are fits to the temporally and spacially integrated forms of eq A.3 in the Appendix. We calculate a cis formation quantum yield of $R_{\text{c}} = 0.12 \pm 0.02$ for NMA and $R_{\text{c}} = 0.075 \pm 0.01$ for Gly-Gly. The NMA R_{c} closely agrees with our previous measurement for 218 nm excitation.[17]

We assume a Gaussian laser intensity temporal profile with a value of $\sigma = 16$ ns, and we measured an approximately Gaussian spatial intensity distribution with $\sigma = 45 \pm 2$ μm. We assume here that $K = K' = 0$, because they are at least 100-fold smaller than k_{L} and k_{L}' for the excitation fluxes used here. We calculated k_{L} and k_{L}' values from the incident laser flux value and the trans and cis molar absorptivities.

We measured 206.5 nm molar absorptivities of $(1.1 \pm 0.05) \times 10^3$ M^{-1} cm^{-1} for *trans*-NMA and $(3.3 \pm 0.1) \times 10^3$ M^{-1} cm^{-1} for *trans*-Gly-Gly. The power dependence of the *cis*-NMA concentration is also governed by the ratio of k_{L} to k_{L}'. From the fits in Figure 5, we found that the ratio of cis excitation to trans excitation is 1.8 for NMA and 2.2 for Gly-Gly, from which we estimate 206.5 nm molar absorptivities of $(2.0 \pm 0.2) \times 10^3$ M^{-1} cm^{-1} for *cis*-NMA and $(7.1 \pm 0.8) \times 10^3$ M^{-1} cm^{-1} for *cis*-Gly-Gly. The molar absorptivity of *cis*-NMA agrees very well to that we estimated from the temperature dependence of the absorption spectrum[17] (2.1×10^3 M^{-1} cm^{-1} at 206.5 nm).

Photochemical Degradation Quantum Yields. We determined the photodegradation quantum yields, R_{r}, by monitoring both the absorption and the 206.5 nm Raman spectral bleaching of NMA after extensive illumination by 2.0 mW 206 nm radiation. Each NMA molecule absorbed an average of 21 photons. We obtain similar photodecomposition quantum yields of 0.0027 ± 0.0003 for NMA from the absorption and Raman spectra. The difference absorption spectrum shows a weak new absorption band at 215 nm from a photoproduct while the Raman spectrum shows a band at *ca.* 1375 cm^{-1}. The

(22) (a) Chen, X. G.; Li, P.; Holtz, J. S. W.; Chi, Z.; Pajcini, V.; Asher, S. A.; Kelly, L. A. *J. Am. Chem. Soc.* **1996**, *118*, 9705. (b) Asher, S. A.; Chi, Z.; Li, P. *J. Am. Chem. Soc.* **1997**, submitted. (c) Holtz, J. S. Private communication.

(23) Radzika, A.; Pederson, L.; Wofenden, R. *Biochemistry* **1988**, *27*, 4538.

(24) Jorgensen, W. L.; Gao, J. *J. Am. Chem. Soc.* **1988**, *110*, 4212.

(25) Barker, R. H.; Boudreaux, G. J. *Spectrochim. Acta* **1967**, *23A*, 727.

(26) Bosco, S. R.; Cirillo, A.; Timmons, R. B. *J. Am. Chem. Soc.* **1969**, *91*, 3140.

(27) Pilling, M. J. *Reaction Kinetics*; Clarendon Press: Oxford, U.K., 1975.

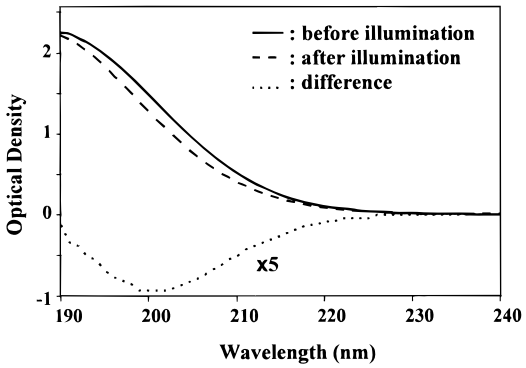

Figure 6. Absorption spectra of Gly-Gly before and after illumination by 2 mW CW, 206.5 nm laser light for 80 min, and the difference spectrum. The sample concentration is 0.35 mM, and the sample volume is 1.5 mL. The sample was stirred during illumination.

photoproduct may be *N*-methylformamide, since previous NMA 200−250 nm photolysis studies demonstrated formation of $CONHCH_3$ free radicals.[26]

Gly-Gly photochemistry was more extensive and complex compared to NMA.[28] The absorption difference spectrum (Figure 6) shows the clear presence of photoproduct absorption. We determined a photodecomposition quantum yield of 0.022 ± 0.003 from the 206 nm Raman spectrum of extensively illuminated Gly-Gly.

The photochemical degradation quantum yield we measure for Gly-Gly is much smaller than that determined by Hill et al.,[28] who used a low-pressure mercury lamp for their quantum yield measurements. The simplest conclusion is that Hill et al. photolysis results derived from the shorter wavelength 185 nmHg UV excitation which resulted in an increased photodegradation quantum yield; Hill et al.[28] presumed that this short excitation wavelengths would be absorbed by oxygen and the impurities in the cooling water. The 254 nm standard mercury excitation is insignificantly absorbed by Gly-Gly.

Ground State Isomerization Activation Barrier. We determined the activation barrier for the ground state trans−cis photoisomerization by measuring the temperature dependence of the value of *K*, which we determined by measuring the sample translation rate dependence of the cis concentration. The experimental conditions utilized ca. 0.45 mW, 206 nm CW laser excitation with a laser beam spot diameter of 90 μm. Given the measured absorption cross sections we calculate excitation rates of $k_L = 34\ s^{-1}$, and $k_L' = 60\ s^{-1}$ at the center of the laser beam, for *trans*-NMA and *trans*-Gly-Gly, respectively.

Figure 7 plots the average concentrations of *cis*-NMA and *cis*-Gly-Gly as a function of the sample translation rate at 22 °C and ca. 70 °C. The solid curves are fits to our three-state model (see Appendix) which extract the ground state isomerization rates, $K = 2.3 \pm 0.3\ s^{-1}$ at 22 °C and $K = 35 \pm 5\ s^{-1}$ at 72 °C for NMA, and $14 \pm 2\ s^{-1}$ at 22 °C and $88 \pm 14\ s^{-1}$ at 70 °C for Gly-Gly. The cis to trans isomerization rates increase significantly with temperature.

We determined the activation barrier for ground state isomerization by examining the temperature dependence of the rate constants.

$$K = K_0 \exp(-E_b/RT) \qquad (3)$$

where E_b is the activation barrier energy of conversion from the cis to the trans amide forms and K_0 is a prefactor.

Figure 8 shows the dependence of ln(*K*) on 1/*T* for NMA and Gly-Gly. The solid lines are the least-squares best fits. The

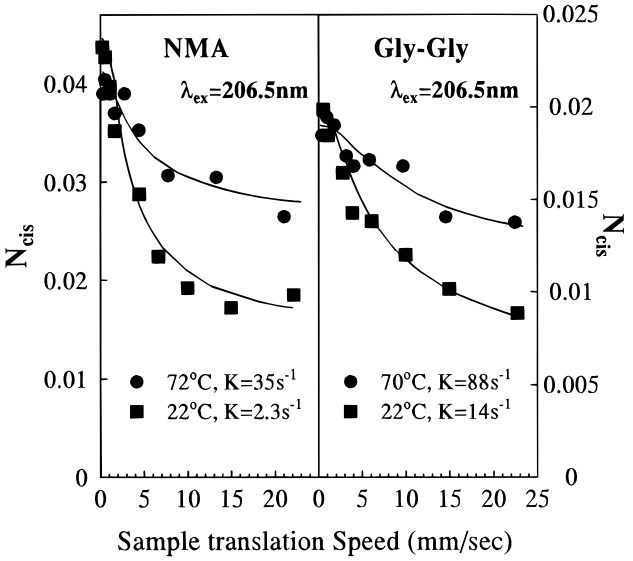

Figure 7. Concentration of *cis*-NMA and *cis*-Gly-Gly as a function of sample translation speed (206.5 nm excitation). The solid curves are the least-squares best fit based on the three-state model, which extracts the isomerization rates from the cis to the trans forms.

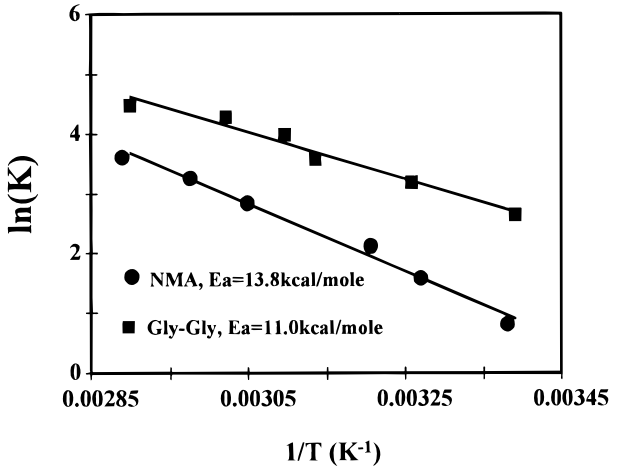

Figure 8. Plot of the natural log of the isomerization rate of the cis form to the trans form versus 1/*T* for NMA and Gly-Gly. The solid lines are linear least-square fits, from which we extract activation barrier heights for the isomerization.

trans to cis conversion activation energy is calculated from

$$E_a = E_b + \Delta G \qquad (4)$$

where ΔG is the Gibbs free energy difference between the ground state cis and trans forms. We calculate an activation barrier energy of $E_a = 13.8 \pm 0.8$ kcal/mol for NMA in water, which is within the range of theoretically calculated **vacuum phase** amide activation energies[1,4,6] and not far below the 16 kcal/mol value measured by NMR for *o*-methylformanilide in chloroform.[16] Our value is, however, ca. 5 kcal/mol lower than that of formamide in organic solution and 9 kcal/mol less than for formamide in water.[11,12]

The differences between the values we measured and that for the other amides probably result from the structural differences which determine energetics of the torsional energies. The torsional barrier energies depend on the extent of double bond character of the C(O)−N bond which strongly depends upon the charge at the carbonyl carbon. This is likely to differ significantly between hydrogen- and methyl-substituted amides.

We obtain values for the Arrenenius prefactors of $K_0 = 4.96 \times 10^8\ s^{-1}$ for NMA and $K_0 = 1.0 \times 10^7\ s^{-1}$ for Gly-Gly. Under

(28) Hill, R. R.; Coyle, J. D.; Birch, D.; Dawe, E.; Jeffs, G. E.; Randall, D.; Stec, I.; Stevenson, T. M. *J. Am. Chem. Soc.* **1991**, *113*, 1805.
(29) Miller, R. J. *Ann. Rev. Phys. Chem.* **1991**, *42*, 581.

the simplest assumptions the rate prefactor is given by[27] $K_0 = \nu_0 \exp(\Delta S^{\ddagger}/R)$, where $\Delta S^{\ddagger}$ is the activation entropy and ν_0 is frequency factor. Using a typical torsional vibrational frequency ($\sim$200 cm^{-1}), we obtain activation entropies of -19 cal/(mol K) for NMA and -26 cal/(mol K) for Gly-Gly. It is interesting that these values are much larger than those found for formamide in organic solution.[11]

Conclusions

We report the first measurements of the activation barrier for trans−cis isomerization of secondary peptides such as *N*-methylacetamide (NMA) and glycylglycine (Gly-Gly) in aqueous solution. We used resonance Raman spectroscopy to measure the temperature dependence of the ground state cis−trans isomerization rates of aqueous NMA and Gly-Gly and have determined the trans to cis activation barrier energies of $E_a = 13.8 \pm 0.8$ kcal/mol for NMA and $E_a = 11.0 \pm 0.7$ kcal/mol for Gly-Gly. We also determined the Gibbs free energy gap, ΔG, between cis and trans NMA and Gly-Gly from the temperature dependence of the trans and cis amide Raman amide band intensities; $\Delta G = 2.6 \pm 0.4$ kcal/mol for NMA, and $\Delta G = 3.1 \pm 0.5$ kcal/mol for Gly-Gly. The different activation barriers of NMA and Gly-Gly demonstrate that the activation barrier height is a function of the amide substituents and presumably depends on the hydrogen bonding of these substituents to the aqueous environment.

Acknowledgment. We gratefully acknowledge support from NIH Grant R01GM30741-13 to S.A.A. We also thank Ms. Janet Holtz, Prof. David Waldeck, Prof. Pam Aker, and Prof. Kenneth Jordan for helpful discussions.

Appendix

I. The Three-State Model. To describe the photochemical dynamics between the cis and trans amides, we use the simple three-state model shown in Figure 2. In this model the amide isomerization reaction coordinate is restricted to one dimension along the CN bond axis. K and K' are the ground state thermal isomerization rates of the cis and trans amides, respectively, and k_L and k_L' are the trans and cis form photoexcitation rates from the ground states to the excited state, which are the product of the absorption cross section and pump laser photon flux. k_t and k_c are the relaxation rates back to the trans and cis ground state forms. k_r is the excited state photochemical degradation rate,[28] which depletes the sample concentration. Because the excited state relaxation rates are very fast (picoseconds to femtoseconds[29]), we can assume a single excited state.

Isomerization occurs both photochemically and through a ground state thermal pathway. The population in each state can be determined by

$$\frac{dN_t}{dt} = -(k_L + K')N_t + k_t N_{ex} + KN_c$$

$$\frac{dN_c}{dt} = K'N_t + k_c N_{ex} - (k_L' + K)N_c$$

$$\frac{dN_{ex}}{dt} = k_L N_t - (k_t + k_c + k_r)N_{ex} + k_L' N_c \qquad \text{(A.1)}$$

At the limit of low photon excitation rates, k_L and $k_L' \rightarrow 0$, the population ratio should be given by the Boltzmann distribution:

$$\left.\frac{N_{cis}}{N_{trans}}\right|_{k_L, k_L' \rightarrow 0} = \frac{K'}{K} = \exp(-\Delta G/RT) \qquad \text{(A.2)}$$

where ΔG is the Gibbs energy difference between the cis and trans amide ground state forms and $R = 1.987$ cal/mol is the gas constant.

In general, k_t, k_c, and k_r (picoseconds to femtosecond) are much faster than k_L and k_L' (which are on the microsecond time scale for pulsed laser excitation with the incident laser intensity used here and are on the millisecond time scale for the CW laser excitation used here), and K and K' are on the millisecond time scale. Thus, the excited state population is very small compare to the cis and trans ground states. The kinetics of the cis form and trans form obey

$$\frac{dN_t}{dt} = -[(1 - R_t)k_L + K']N_t + (R_t k_L' + K)N_c$$

$$\frac{dN_c}{dt} = (K' + R_c k_L)N_t - [(1 - R_c)k_L' + K]N_c \qquad \text{(A.3)}$$

R_c, R_t, and R_r are the excited state quantum yields for formation of the cis, trans, and degradation photoproducts, $R_c = k_c/(k_c + k_r + k_t)$, $R_t = k_t/(k_c + k_r + k_t)$, and $R_r = k_r/(k_c + k_r + k_t)$. For the pulsed laser excitation case, K and K' are negligible.

Pulsed Laser Excitation. High nanosecond pulse energy excitation (k_L, $k_L' \gg K$, K') can result in a photochemical steady state, if k_r is small compared to k_c and k_t. Thus

$$R = \frac{k_c}{k_t} = \frac{\sigma_c N_c^{st}}{\sigma_t N_t^{st}} \approx \frac{\sigma_c N_c^{st}}{\sigma_t (1 - N_c^{st})} \qquad \text{(A.4)}$$

where σ_t and σ_c are the absorption cross sections of the trans and cis form, and N_c^{st} and N_t^{st} are steady state populations of the cis form and trans form. The quantum yield for the cis form is

$$R_c = \frac{R(1 - R_r)}{(1 + R)}$$

CW Laser Excitation. Translation of the sample solution through the laser beam at a speed v results in a time dependence of the apparent laser intensity. This results in a time dependence for the apparent molecular excitation rate, $k_L(x = vt, y, z)$:

$$k_L(x,y,z) = \sigma_A I(x,y,z)/h\nu \qquad \text{(A.5)}$$

where σ_A is the absorption cross section, $I(x,y,z)$ is the laser intensity profile, h is Planck's constant, and ν is the laser frequency.

The cis population distribution $N_{cis}(x,y,z)$ can be calculated from eq A.3, if R_c, R_t, R_r, K, K', $I(x,y,z)$, and the absorption cross sections for cis and trans forms, σ_A^c and σ_A^t are known. The Raman intensity is given by

$$I_R^{cis} \propto \sigma_R^{cis} \int N_c(x,y,z)\, I_L(x,y,z)\, dx\, dy\, dz \qquad \text{(A.6)}$$

And the spatially averaged cis amide population in the excitation volume can be calculated from

$$\langle N_c \rangle = \frac{I_R^{cis}}{\sigma_R^{cis} \int I_L(x,y,z)\, dx\, dy\, dz} \qquad \text{(A.7)}$$

or

$$\langle N_c \rangle = \frac{\int N_{cis}(x,y,z)\, I_L(x,y,z)\, dx\, dy\, dz}{\int I_L(x,y,z)\, dx\, dy\, dz} \qquad \text{(A.8)}$$

In the data analysis, we used eq A.8 to calculate the cis concentration from the Raman intensities. We also used eq A.3 to simulate the cis spatial distribution as functions of the sample translation speed and the ground state conversion rate, K, and extracted K by least-squares fitting.

JA962058C